

See discussions, stats, and author profiles for this publication at: <https://www.researchgate.net/publication/49633964>

Substitution of the Terminal Chloride Ligands of $[\text{Re}_6\text{S}_8\text{Cl}_6](4-)$ with Triethylphosphine: Photophysical and Electrochemical Properties of a New Series of $[\text{Re}_6\text{S}_8](2+)$ Based Clusters

ARTICLE *in* INORGANIC CHEMISTRY · DECEMBER 2010

Impact Factor: 4.76 · DOI: 10.1021/ic101348h · Source: PubMed

CITATIONS

15

READS

4

7 AUTHORS, INCLUDING:



David L Cedeño

Millennium Pain Center

41 PUBLICATIONS 419 CITATIONS

SEE PROFILE



Jessica L Durham

Stony Brook University

8 PUBLICATIONS 39 CITATIONS

SEE PROFILE

Substitution of the Terminal Chloride Ligands of $[\text{Re}_6\text{S}_8\text{Cl}_6]^{4-}$ with Triethylphosphine: Photophysical and Electrochemical Properties of a New Series of $[\text{Re}_6\text{S}_8]^{2+}$ Based Clusters

Lisa F. Szczepura,^{*,†} David L. Cedeño,^{*,†} Dean B. Johnson,[†] Robert McDonald,[†] Stanley A. Knott,[†] Kristen M. Jeans,[†] and Jessica L. Durham[†]

[†]Department of Chemistry, Illinois State University, Normal, Illinois 61790-4160, United States, and

^{*}Department of Chemistry, University of Alberta, Edmonton, Alberta T6G 2G2, Canada

Received July 6, 2010

A systematic substitution of the terminal chlorides coordinated to the hexanuclear cluster $[\text{Re}_6\text{S}_8\text{Cl}_6]^{4-}$ has been conducted. The following complexes: $[\text{Re}_6\text{S}_8(\text{PET}_3)\text{Cl}_5]^{3-}$ (**1**), *cis*- (**cis-2**) and *trans*- $[\text{Re}_6\text{S}_8(\text{PET}_3)_2\text{Cl}_4]^{2-}$ (**trans-2**), *mer*- (**mer-3**) and *fac*- $[\text{Re}_6\text{S}_8(\text{PET}_3)_3\text{Cl}_3]^{-}$ (**fac-3**), and *cis*- (**cis-4**) and *trans*- $[\text{Re}_6\text{S}_8(\text{PET}_3)_4\text{Cl}_2]$ (**trans-4**) were synthesized and fully characterized. Compared to the substitution of the halide ligands of the related $[\text{Re}_6\text{S}_8\text{Br}_6]^{4-}$ and $[\text{Re}_6\text{Se}_8\text{I}_6]^{3-}$ clusters, the chloride ligands are slower to substitute which allowed us to prepare the first monophosphine cluster (**1**). In addition, the synthesis of **fac-3** was optimized by using **cis-2** as the starting material, which led to a significant increase in the overall yield of this isomer. Notably, we observed evidence of phosphine isomerization taking place during the preparation of the facial isomer; this was unexpected based on the relatively inert nature of the Re–P bond. The structures of Bu_4N^+ salts of **trans-2**, **mer-3**, and **fac-3** were determined using X-ray crystallography. All compounds display luminescent behavior. A study of the photophysical properties of these complexes includes measurement of the excited state lifetimes (which ranged from 4.1–7.1 μs), the emission quantum yields, the rates of radiative and non-radiative decay, and the rate of quenching with O_2 . Quenching studies verify the triplet state nature of the excited state.

Introduction

Octahedral hexanuclear clusters with the general formula $[\text{M}_6\text{X}_8\text{L}_6]^{n+}$ or $[\text{M}_6\text{Q}_8\text{L}_6]^{n+}$ (X = halide and Q = chalcogenide) have attracted a great deal of attention over the past

20 years.^{1–3} These facially bridging cluster complexes are well-known for their remarkable photophysical and electrochemical properties.^{4–6} The regular geometry of these clusters, and their edge bridged analogues ($[\text{M}_6\text{X}_{12}]^{n+}$), possess non-fluxional ligands and have a robust core, these properties make them attractive as building blocks in the preparation of new materials. To date, a number of new one-dimensional (chains), two-dimensional (sheets), and three-dimensional (3D, framework solids) polymers have been prepared from these types of discrete octahedral cluster complexes.^{7–11} Most of these contain $[\text{M}_6\text{Q}_8(\text{CN})_6]^{n-}$ (M = Re, Mo, or W; Q = S, Se, or Te) and take advantage of the ability of cyanide ligands to bridge metal centers and the presence of additional metal ions to generate materials that are analogous to Prussian blue.⁸ However, other types of 3D solids have been prepared, along with some

^{*}To whom correspondence should be addressed. E-mail: lfszcze@ilstu.edu (L.F.S.), dcedeno@ilstu.edu (D.L.C.).

(1) Review articles: (a) Perrin, A.; Perrin, C. *J. Clust. Sci.* **2009**, *20*, 1–7. (b) Welch, E. J.; Long, J. R. *Prog. Inorg. Chem.* **2005**, *54*, 1–45. (c) Gabriel, J.-C. P.; Boubekur, K.; Uriel, S.; Batail, P. *Chem. Rev.* **2001**, *101*, 2037–2066. (d) Prokopuk, N.; Shriver, D. F. *Adv. Inorg. Chem.* **1998**, *46*, 1–49. (e) Fedorov, V. E.; Mironov, N. G.; Naumov, N. G.; Sokolov, M. N.; Fedin, V. P. *Russ. Chem. Rev.* **2007**, *76*, 529–552. (f) Saito, T. *Adv. Inorg. Chem.* **1997**, *44*, 45–91.

(2) (a) Maverick, A. W.; Gray, H. B. *J. Am. Chem. Soc.* **1981**, *103*, 1298–1300. (b) Saito, T.; Yamamoto, N.; Yamagata, T.; Imoto, H. *J. Am. Chem. Soc.* **1988**, *110*, 1646–1647. (c) Long, J. R.; Williamson, A. S.; Holm, R. H. *Angew. Chem., Int. Ed. Engl.* **1995**, *34*, 226–229. (d) Long, J. R.; McCarty, L. S.; Holm, R. H. *J. Am. Chem. Soc.* **1996**, *118*, 4603–4616. (e) Mironov, Y. V.; Pell, M. A.; Ibers, J. A. *Inorg. Chem.* **1996**, *35*, 2709–2710.

(3) (a) Robinson, L. M.; Bain, R. L.; Shriver, D. F.; Ellis, D. E. *Inorg. Chem.* **1995**, *34*, 5588–5596. (b) Alvarez-Thon, L.; Hernandez-Acevedo, L.; Arratia-Pérez, R. *J. Chem. Phys.* **2001**, *115*, 726–730. (c) Gautier, R.; Furet, E.; Halet, J.-F.; Lin, Z.; Saillard, J.-Y.; Zu, Z. *Inorg. Chem.* **2002**, *41*, 796–804. (d) Deluzet, A.; Duclausaud, H.; Sautet, P.; Borshch, S. A. *Inorg. Chem.* **2002**, *41*, 2537–2542.

(4) (a) Gray, T. G.; Rudzinski, C. M.; Nocera, D. G.; Holm, R. H. *Inorg. Chem.* **1999**, *38*, 5932–5933. (b) Kitamura, N.; Ueda, Y.; Ishizaka, S.; Yamada, K.; Aniya, M.; Sasaki, Y. *Inorg. Chem.* **2005**, *44*, 6308–6313.

(5) (a) Yoshimura, T.; Ishizaka, S.; Umakoshi, K.; Sasaki, Y.; Kim, H.-B.; Kitamura, N. *Chem. Lett.* **1999**, 697–698. Yoshimura, T.; Umakoshi, K.; Sasaki, Y.; Sykes, A. G. *Inorg. Chem.* **1999**, *38*, 5557–5564.

(6) (a) Maverick, A. W.; Najdzionek, J. S.; MacKenzie, D.; Nocera, D. G.; Gray, H. B. *J. Am. Chem. Soc.* **1983**, *105*, 1878–1882. (b) Nocera, D. G.; Gray, H. B. *J. Am. Chem. Soc.* **1984**, *106*, 824–825. (c) Guilbaud, C.; Deluzet, A.; Domercq, B.; Molinié, P.; Coulon, C.; Boubekur, K.; Batail, P. *Chem. Commun.* **1999**, 1867–1868. (d) Baudron, S. A.; Batail, P.; Coulon, C.; Clerac, R.; Canadell, E.; Laukhin, V.; Melzi, R.; Wzietek, P.; Jerome, P.; Auban-Senzier, P.; Ravy, S. *J. Am. Chem. Soc.* **2005**, *127*, 11785–11797. (e) Gray, T. G.; Rudzinski, C. M.; Meyer, E. E.; Nocera, D. G. *J. Phys. Chem. A* **2004**, *108*, 3238–3243. (f) Gray, T. G.; Rudzinski, C. M.; Meyer, E. E.; Holm, R. H.; Nocera, D. G. *J. Am. Chem. Soc.* **2003**, *125*, 4755–4770.

(7) (a) Brnicevic, N.; Mustovic, F.; McCarty, R. E. *Inorg. Chem.* **1988**, *27*, 4532–4535. (b) Xie, X.; Hughbanks, T. *Angew. Chem., Int. Ed.* **1999**, *38*, 1777–1779.

modular units which can be envisioned as building blocks for the preparation of metal–organic framework solids.^{9,10} These are of special interest because combining different modules could lead to greater control of the properties of the resulting solid-state materials. There has even been some success in taking discrete cluster complexes with more labile ligands and condensing them to form clusters bridged together in a manner similar to that found in ternary Chevrel phase materials ($M'Mo_6S_8$) which are known for their superconducting properties.^{11,12}

One important factor of using discrete hexanuclear clusters as modular building blocks in the design and preparation of new materials is the substitution (or removal) of the terminal ligands coordinated to the cluster core. Substitution of all six terminal ligands is by far the most common for discrete hexanuclear cluster complexes containing six terminal ligands.¹³ Prior to 1997, the only examples of $[M_6X_8L_6]^{n+}$ or $[M_6Q_8L_6]^{n+}$ clusters containing mixed-terminal ligands were those formed from Mo_6X_{12} ($X = Br, Cl, I$).¹⁴ Mo_6Cl_{12} is considered as a polymeric material consisting of $[Mo_6Cl_8]^{4+}$ cores bridged together via axial chloride ligands; these bridging interactions are readily disrupted by Lewis bases (L) leading to the formation of 4:2 site-differentiated *cis*- and *trans*- $[Mo_6(\mu_3-Cl)_8Cl_4L_2]$ complexes.^{14–16} Notably, Holm and co-workers were the first to demonstrate control over substitution of the terminal halide ligands of a facially bridged hexanuclear cluster core when they reacted $[Re_6Se_8I_6]^{3-}$ or $[Re_6S_8Br_6]^{4-}$ with PEt_3 , generating $[Re_6Se_8(PEt_3)_nI_{6-n}]^{4-n}$ ($n = 3–6$) and $[Re_6S_8(PEt_3)_nBr_{6-n}]^{4-n}$ ($n = 2–6$), respectively.^{17,18} Although mixtures of

substitution products were reported, the inert nature of rhenium allowed for the enrichment or optimization of one product over another by changing the number equivalents of donor ligand and/or the reaction conditions (time and temperature). The various substitution products, including different isomers, can usually be separated using column chromatography. Because of the strong Re–P bond, subsequent substitution of the remaining halide ligands (often using a silver salt) enables the preparation of other mixed-ligand systems (e.g., reaction of $[Re_6Se_8(PEt_3)_5I]^+$ with $AgBF_4$ in MeCN leads to the formation of $[Re_6Se_8(PEt_3)_5(MeCN)]^{2+}$).¹⁷ Therefore, site-differentiation of the terminal halide ligands of the $[Re_6Q_8X_6]^{4-}$ clusters, allows for the generation of a much wider range of cluster complexes since nitriles are often readily substituted by other ligands.^{19,20}

In an effort to learn more about the substitution properties of the rhenium based cluster cores, we set out to investigate the substitution properties of the analogous $[Re_6S_8Cl_6]^{4-}$ cluster. Although some substitution reactions involving this compound have been reported, the studies focused on the physical properties of the final compounds (all of which contained N-donor ligands) as opposed to examining the details of the substitution reactions themselves.^{5b,21} This study focuses on substitution of the terminal chloride ligands of $[Re_6S_8Cl_6]^{4-}$ with PEt_3 . In addition to a comparison with previous studies, we discuss the scope of substitution, evidence of phosphine isomerization, and a method of optimizing the yield of *fac*- $[Re_6S_8(PEt_3)_3Cl_3]^-$. We also report on the electrochemical and optical properties of this new family of clusters, including quenching studies by oxygen involving the $[Re_6Q_8]^{2+}$ based cluster complexes.

Experimental Section

General Methods and Materials. The rhenium cluster complex starting material, $(Bu_4N)_4[Re_6S_8Cl_6]$, was prepared according to a previously published method.^{2d} Rhenium metal and rhenium(V) chloride were purchased from Cerac. Air and moisture-sensitive materials were stored under argon in an inert atmosphere glovebox. All newly prepared compounds are yellow-orange. 1H (and ^{31}P) spectra were recorded using a 400 MHz (162 MHz) Varian Mercury or a 500 MHz (202.5 MHz) Bruker Avance III NMR spectrometer equipped with a tunable probe. All ^{31}P spectra were proton decoupled, unless otherwise noted, and externally referenced to an 85% (w/w) H_3PO_4 solution. Cyclic voltammetric measurements were carried out in anhydrous CH_3CN or CH_2Cl_2 (0.2 M Bu_4NBF_4), at a scan rate of 100 mV/s, using a BAS CV50W voltammetric analyzer. A conventional three electrode cell consisting of a platinum disk working electrode, a platinum wire auxiliary electrode, and an $Ag/AgNO_3$ (0.01 M) reference electrode was used. The ferrocenium/ferrocene couple was observed at 0.087 V versus $Ag/AgNO_3$ in MeCN; consequently, all potentials were referenced to $FeCp_2^+/FeCp_2$ by subtracting 0.087 V from the measured values.²²

$(Bu_4N)_3[Re_6S_8(PEt_3)Cl_3]$ (1). A 400 mg (0.156 mmol) sample of $(Bu_4N)_4[Re_6S_8Cl_6]$ was dissolved in 72 mL of DMF. The solution was sparged with N_2 prior to bringing the solution into the glovebox to add 46 μ L of PEt_3 (0.312 mmol). The solution was stirred at 100 °C for 1.5 h. The solvent was removed, and the

(8) (a) Naumov, N. G.; Virovets, A. V.; Sokolov, M. N.; Artemkina, S. B.; Fedorov, V. E. *Angew. Chem., Int. Ed.* **1998**, *37*, 1943–1945. (b) Bennett, M. V.; Shores, M. P.; Beauvais, L. G.; Long, J. R. *J. Am. Chem. Soc.* **2000**, *122*, 6664–6668. (c) Beauvais, L. G.; Shores, M. P.; Long, J. R. *J. Am. Chem. Soc.* **2000**, *122*, 2763–2772. (d) Jin, S.; DiSalvo, F. J. *Chem. Mater.* **2002**, *14*, 3448–3457. (e) Mironov, Y. V.; Naumov, N. G.; Brylev, K. A.; Efremova, O. A.; Fedorov, V. E.; Hegetschweiler, K. *Angew. Chem., Int. Ed.* **2004**, *43*, 1297–1300. (f) Brylev, K. A.; Mironov, Y. V.; Naumov, N. G.; Fedorov, V. E.; Ibers, J. A. *Inorg. Chem.* **2004**, *43*, 4833–4838. (g) Brylev, K. A.; Naumov, N. G.; Virovets, A. V.; Kim, S.-J.; Fedorov, V. E. *J. Clust. Sci.* **2009**, *20*, 165–176. (h) Naumov, N. G.; Virovets, A. V.; Fedorov, V. E. *J. Struct. Chem.* **2000**, *41*, 499–520. (i) Kim, Y.; Fedorov, V. E.; Kim, S.-J. *J. Mater. Chem.* **2009**, *19*, 7178–7190.

(9) (a) Golden, H. H.; Deng, H.; DiSalvo, F. J.; Frechet, J. M. J.; Thompson, P. M. *Science* **1995**, *268*, 1463–1466. (b) Yuan, M.; Ulgut, B.; McGuire, M.; Takada, K.; DiSalvo, F.; Lee, S.; Abruna, H. *Chem. Mater.* **2006**, *18*, 4296–4306. (c) Selby, H. D.; Roland, B. K.; Cole, J. R.; Zheng, Z. *Macromol. Symp.* **2004**, *209*, 23–39.

(10) (a) Zheng, A.; Gray, T. G.; Holm, R. H. *Inorg. Chem.* **1999**, *38*, 4888–4895. (b) Selby, H. D.; Zheng, Z.; Gray, T. G.; Holm, R. H. *Inorg. Chim. Acta* **2001**, *312*, 205–209. (c) Roland, B. K.; Selby, H. D.; Carducci, M. D.; Zheng, Z. *J. Am. Chem. Soc.* **2002**, *124*, 3222. (d) Roland, B. K.; Flora, W. H.; Armstrong, N. R.; Zheng, Z. *C. R. Chimie* **2005**, *8*, 1798–1807.

(11) (a) Beers, W. W.; McCarley, R. E. *Inorg. Chem.* **1985**, *24*, 468–471. (b) Hilsenbeck, S. J.; McCarley, R. E.; Goldman, A. I. *Chem. Mater.* **1995**, *7*, 499–506. (c) Zheng, Z.; Holm, R. H. *Inorg. Chem.* **1997**, *36*, 5173–5178.

(12) (a) Chevrel, R.; Gougeon, P.; Potel, M.; Sergent, M. *J. Solid State Chem.* **1985**, *57*, 25–33. (b) Chevrel, R.; Hirrien, M.; Sergent, M. *Polyhedron* **1986**, *5*, 87–94.

(13) (a) Johnston, D. H.; Gaswick, D. C.; Lonergan, M. C.; Stern, C. L.; Shriver, D. F. *Inorg. Chem.* **1992**, *31*, 1869–1873. (b) Hilsenbeck, S. J.; Young, V. G.; McCarley, R. E. *Inorg. Chem.* **1994**, *33*, 1822–1832. (c) Jin, S.; Zhou, R.; Scheuer, E. M.; Adamchuk, J.; Rayburn, L. L.; DiSalvo, F. J. *Inorg. Chem.* **2001**, *40*, 2666–2674. (14) Saito, T.; Nishida, M.; Yamagata, T.; Yamagata, Y.; Yamaguchi, Y. *Inorg. Chem.* **1986**, *25*, 1111–1117.

(15) (a) Cotton, F. A.; Curtis, N. F. *Inorg. Chem.* **1965**, *4*, 241–244. (b) Schäfer, H.; Plautz, H.; Abel, H.-J.; Lademann, D. Z. *Anorg. Allg. Chem.* **1985**, *526*, 168–176. (c) Kraft, J.; Schäfer, H. Z. *Anorg. Allg. Chem.* **1985**, *524*, 137–143.

(16) Guggenberger, J.; Sleight, A. W. *Inorg. Chem.* **1969**, *8*, 2041–2049. (17) Zheng, Z.; Long, J. R.; Holm, R. H. *J. Am. Chem. Soc.* **1997**, *119*, 2163–2171.

(18) Willer, M. W.; Long, J. R.; McLauchlan, C. C.; Holm, R. H. *Inorg. Chem.* **1998**, *37*, 328–333.

(19) Endres, H. In *Comprehensive Coordination Chemistry I*; Wilkinson, G., Ed.; Pergamon Press: New York, 1987; pp 261–267.

(20) Wang, R.; Zheng, Z. *J. Am. Chem. Soc.* **1999**, *121*, 3549–3550.

(21) (a) Yoshimura, T.; Umakoshi, K.; Sasaki, Y.; Ishizaka, S.; Kim, H.-B.; Kitamura, N. *Inorg. Chem.* **2000**, *39*, 1765–1772. (b) Yoshimura, T.; Suo, C.; Tsuge, K.; Ishizaka, S.; Nozaki, K.; Sasaki, Y.; Kitamura, N.; Shinohara, A. *Inorg. Chem.* **2010**, *49*, 531–540.

(22) Pavlishchuk, V. V.; Addison, A. W. *Inorg. Chim. Acta* **2000**, *198*, 97–102.

residue dissolved in 6 mL of CH_2Cl_2 and filtered through Celite. The filtrate was concentrated and precipitated using Et_2O . The crude solid was purified by column chromatography on silica gel. An impurity was eluted using a 7:2 $\text{CH}_2\text{Cl}_2/\text{CH}_3\text{CN}$ mixture, then the product was eluted using a 2:1 $\text{CH}_2\text{Cl}_2/\text{CH}_3\text{CN}$ mixture. The product band was reduced to dryness by rotary evaporation, and a solid was obtained by reprecipitation using $\text{CH}_2\text{Cl}_2/\text{Et}_2\text{O}$. Crystals were obtained by vapor diffusion crystallization using acetone and toluene (yield: 160.0 mg, 43%). ^1H NMR (CD_3CN , ppm): 0.97 (36H, t, $\text{N}(\text{CH}_2\text{CH}_2\text{CH}_2\text{CH}_3)_4^+$), 1.11 (9H, m, $\text{P}(\text{CH}_2\text{CH}_3)_3$), 1.37 (24H, m, $\text{N}(\text{CH}_2\text{CH}_2\text{CH}_2\text{CH}_3)_4^+$), 1.61 (24H, m, $\text{N}(\text{CH}_2\text{CH}_2\text{CH}_2\text{CH}_3)_4^+$), 2.08 (6H, m, $\text{P}(\text{CH}_2\text{CH}_3)_3$), 3.10 (24H, t, $\text{N}(\text{CH}_2\text{CH}_2\text{CH}_2\text{CH}_3)_4^+$). ^{31}P $\{^1\text{H}\}$ NMR (CD_3CN , ppm): -13.12. UV/vis (CH_3CN) nm (ϵ in $\text{M}^{-1}\text{cm}^{-1}$): 225 (7080), 267 (2610). MS (ESI(-)): m/z 834.6 ($[\text{Re}_6\text{S}_8(\text{PET}_3)_3\text{Cl}_3]^{2-}$). Anal. Calcd for $\text{C}_{54}\text{H}_{123}\text{N}_3\text{P}_3\text{Cl}_3\text{Re}_6\text{S}_8 \cdot \text{H}_2\text{O}$: C, 26.86; H, 5.18; N, 1.74. Found: C, 26.51; H, 5.18; N, 1.83.

(Bu_4N) $_2$ $[\text{Re}_6\text{S}_8(\text{PET}_3)_2\text{Cl}_4]$. A 750.3 mg (0.294 mmol) sample of $(\text{Bu}_4\text{N})_4[\text{Re}_6\text{S}_8\text{Cl}_6]$ was weighed out and dissolved in 135 mL of DMF. The solution was sparged with N_2 and brought into the glovebox. 120.0 μL (0.880 mmol) of PET_3 was added to the solution, and the solution was heated at 100 $^\circ\text{C}$ for 8 h and then evaporated to dryness in vacuo. The residue was dissolved with 15 mL of DMF; then 40 mL of deionized H_2O was added and upon chilling a precipitate formed and was isolated.

***cis*-(Bu_4N) $_2$ $[\text{Re}_6\text{S}_8(\text{PET}_3)_2\text{Cl}_4]$ (*cis*-2).** This material was collected by adding 10 mL of acetone to the solid. The mixture was filtered, and the filtrate was evaporated to dryness using rotary evaporation. The resulting residue was collected as *cis*-(Bu_4N) $_2$ $[\text{Re}_6\text{S}_8(\text{PET}_3)_2\text{Cl}_4]$ (yield: 580.5 mg, 88.4%). ^1H NMR (CDCl_3 , ppm): 0.99 (24H, t, $\text{N}(\text{CH}_2\text{CH}_2\text{CH}_2\text{CH}_3)_4^+$), 1.11 (18H, m, $\text{P}(\text{CH}_2\text{CH}_3)_3$), 1.53 (16H, m, $\text{N}(\text{CH}_2\text{CH}_2\text{CH}_2\text{CH}_3)_4^+$), 1.65 (16H, m, $\text{N}(\text{CH}_2\text{CH}_2\text{CH}_2\text{CH}_3)_4^+$), 2.10 (12H, m, $\text{P}(\text{CH}_2\text{CH}_3)_3$), 3.30 (16H, m, $\text{N}(\text{CH}_2\text{CH}_2\text{CH}_2\text{CH}_3)_4^+$). ^{31}P $\{^1\text{H}\}$ NMR (CDCl_3 , ppm): -15.36. UV/vis (CH_3CN) nm (ϵ in $\text{M}^{-1}\text{cm}^{-1}$): 225 (61,000), 268 sh (18,500). MS (ESI(-)): m/z 1994.0 ($(\text{Bu}_4\text{N})[\text{Re}_6\text{S}_8(\text{PET}_3)_2\text{Cl}_4]^+$). Anal. Calcd for $\text{C}_{44}\text{H}_{102}\text{N}_2\text{P}_2\text{Cl}_4\text{Re}_6\text{S}_8$: C, 23.62; H, 4.60; N, 1.25. Found: C, 23.78; H, 4.63; N, 1.34.

***trans*-(Bu_4N) $_2$ $[\text{Re}_6\text{S}_8(\text{PET}_3)_2\text{Cl}_4]$ (*trans*-2).** This material was collected by adding 10 mL of acetone to the solid to dissolve any remaining *cis*-isomer. The mixture was filtered and the solid was collected as *trans*-(Bu_4N) $_2$ $[\text{Re}_6\text{S}_8(\text{PET}_3)_2\text{Cl}_4]$ (yield: 50.5 mg, 7.69%). ^1H NMR (CD_2Cl_2 , ppm): 1.01 (24H, t, $\text{N}(\text{CH}_2\text{CH}_2\text{CH}_2\text{CH}_3)_4^+$), 1.17 (18H, m, $\text{P}(\text{CH}_2\text{CH}_3)_3$), 1.50 (16H, m, $\text{N}(\text{CH}_2\text{CH}_2\text{CH}_2\text{CH}_3)_4^+$), 1.63 (16H, m, $\text{N}(\text{CH}_2\text{CH}_2\text{CH}_2\text{CH}_3)_4^+$), 2.19 (12H, m, $\text{P}(\text{CH}_2\text{CH}_3)_3$), 3.21 (16H, m, $\text{N}(\text{CH}_2\text{CH}_2\text{CH}_2\text{CH}_3)_4^+$). ^{31}P $\{^1\text{H}\}$ NMR (CD_2Cl_2 , ppm): -12.96. UV/vis (CH_3CN) nm (ϵ in $\text{M}^{-1}\text{cm}^{-1}$): 223 (57,700), 268 (16,800), 279 sh (15,600). MS (ESI(-)): m/z 1993.5 ($(\text{Bu}_4\text{N})[\text{Re}_6\text{S}_8(\text{PET}_3)_2\text{Cl}_4]^+$). Anal. Calcd for $\text{C}_{44}\text{H}_{102}\text{N}_2\text{P}_2\text{Cl}_4\text{Re}_6\text{S}_8$: C, 23.62; H, 4.60; N, 1.25. Found: C, 23.45; H, 4.63; N, 1.33.

***mer*-(Bu_4N) $[\text{Re}_6\text{S}_8(\text{PET}_3)_3\text{Cl}_3]$ (*mer*-3).** $(\text{Bu}_4\text{N})_4[\text{Re}_6\text{S}_8\text{Cl}_6]$ (501.0 mg, 0.196 mmol) was dissolved in 128 mL of DMF. The solution was sparged with N_2 and taken into the glovebox whereupon 80.0 μL (0.588 mmol) of PET_3 was added. The solution was heated at reflux for 18 h and evaporated to dryness in vacuo. The residue was dissolved with 15 mL of DMF, and 15 mL of deionized H_2O was added to cause a precipitate to fall out. The solid was collected via filtration and dissolved using a minimal amount of CH_3CN . The solution was placed in a beaker, covered, and allowed to stand at room temperature for 2 d. A solid formed that was collected via filtration. This solid was a mixture of products, and was purified via chromatography using silica gel as the solid support. The desired product was collected as the third band which was eluted with a 8:1 $\text{CH}_2\text{Cl}_2/\text{CH}_3\text{CN}$ mixture (the first two bands were eluted with the same solvents in a 10:1 and 15:1 ratio, respectively), yield: 115.7 mg, 25.1%. ^1H NMR (CDCl_3 , ppm): 0.97 (12H, t, Bu_4N^+), 1.11 (27H, m, $\text{P}(\text{CH}_2\text{CH}_3)_3$), 1.49 (8H, m, Bu_4N^+), 1.61 (8H, m, Bu_4N^+), 2.05 (6H, m, $\text{P}(\text{CH}_2\text{CH}_3)_3$), 2.13 (12H, m,

$\text{P}(\text{CH}_2\text{CH}_3)_3$), 3.24 (8H, t, Bu_4N^+). ^{31}P $\{^1\text{H}\}$ NMR (CDCl_3 , ppm): -14.46, -17.18. UV/vis (CH_3CN) nm (ϵ in $\text{M}^{-1}\text{cm}^{-1}$): 223 (63,600), 257 sh (18,700), 269 sh (17,000). MS (ESI(-)): m/z 1834.1 ($[\text{Re}_6\text{S}_8(\text{PET}_3)_3\text{Cl}_3]^-$). Anal. Calcd for $\text{C}_{34}\text{H}_{81}\text{NP}_3\text{Cl}_3\text{Re}_6\text{S}_8$: C, 19.66; H, 3.93; N, 0.67. Found: C, 19.38; H, 3.78; N, 0.74.

***fac*-(Bu_4N) $[\text{Re}_6\text{S}_8\text{Cl}_3(\text{PET}_3)_3]$ (*fac*-3).** *cis*-(Bu_4N) $_2$ $[\text{Re}_6\text{S}_8\text{Cl}_4(\text{PET}_3)_2]$ (325.1 mg, 0.145 mmol) was dissolved in 70 mL of DMF whereupon 40 μL of PET_3 (0.2594 mmol) was added to the solution inside the glovebox. The solution was then heated at reflux for 3 h under N_2 . After cooling, the solution was reduced to dryness, and the crude product was dissolved in about 2 mL of CH_2Cl_2 and reprecipitated with Et_2O (yield: 293.8 mg, 97%). This solid contained a mixture of *fac*- and *mer*-(Bu_4N) $[\text{Re}_6\text{S}_8\text{Cl}_3(\text{PET}_3)_3]$. The product was dissolved in CH_2Cl_2 and purified via column chromatography on silica gel. *Mer*-(Bu_4N) $[\text{Re}_6\text{S}_8\text{Cl}_3(\text{PET}_3)_3]$ (*mer*-3) was eluted first with 10:1 $\text{CH}_2\text{Cl}_2/\text{CH}_3\text{CN}$ (yield: 157.7 mg, 52%). ^1H NMR (CDCl_3 , ppm): 0.94 (12H, t, Bu_4N^+), 1.07 (27H, m, $\text{P}(\text{CH}_2\text{CH}_3)_3$), 1.42 (8H, m, Bu_4N^+), 1.57 (8H, m, Bu_4N^+), 2.01 (6H, m, $\text{P}(\text{CH}_2\text{CH}_3)_3$), 2.09 (12H, m, $\text{P}(\text{CH}_2\text{CH}_3)_3$), 3.14 (8H, t, Bu_4N^+). ^{31}P $\{^1\text{H}\}$ NMR (CD_2Cl_2 , ppm): -14.75, -17.08. Anal. Calcd for $\text{C}_{34}\text{H}_{81}\text{NP}_3\text{Cl}_3\text{Re}_6\text{S}_8$: C, 19.66; H, 3.93; N, 0.67. Found: C, 19.65; H, 3.74; N, 0.74. ***fac*-(Bu_4N) $[\text{Re}_6\text{S}_8\text{Cl}_3(\text{PET}_3)_3]$ (*fac*-3).** The second band was the desired product (*fac*-(Bu_4N) $[\text{Re}_6\text{S}_8\text{Cl}_3(\text{PET}_3)_3]$) and was eluted with 5:1 $\text{CH}_2\text{Cl}_2/\text{CH}_3\text{CN}$ (yield: 56.1 mg, 19%). ^1H NMR (CD_2Cl_2 , ppm): 1.02 (12 H, t, Bu_4N^+), 1.11 (27 H, m, $\text{P}(\text{CH}_2\text{CH}_3)_3$), 1.51 (8H, m, Bu_4N^+), 1.66 (8H, m, Bu_4N^+), 2.08 (18H, m, $\text{P}(\text{CH}_2\text{CH}_3)_3$), 3.23 (8H, t, Bu_4N^+). ^{31}P $\{^1\text{H}\}$ NMR (CD_2Cl_2 , ppm): -17.77. UV-vis (CH_3CN) nm (ϵ in $\text{M}^{-1}\text{cm}^{-1}$): 246 (21000), 259 sh (20000). MS (ESI(-)): m/z 1835.5 ($[\text{Re}_6\text{S}_8(\text{PET}_3)_3\text{Cl}_3]^-$). Anal. Calcd for $\text{C}_{34}\text{H}_{81}\text{NP}_3\text{Cl}_3\text{Re}_6\text{S}_8$: C, 19.66; H, 3.93; N, 0.67. Found: C, 19.48; H, 3.84; N, 0.73.

$[\text{Re}_6\text{S}_8\text{Cl}_2(\text{PET}_3)_4]$. $(\text{Bu}_4\text{N})_4[\text{Re}_6\text{S}_8\text{Cl}_6]$ (1.148 g, 0.449 mmol) was dissolved in 180 mL of DMF. The solution was sparged with N_2 and brought into the glovebox, 400 μL of (2.941 mmol) PET_3 was added, and the flask was brought out of the glovebox. The solution was heated at reflux for 3 d, then evaporated to dryness in vacuo. The residue was dissolved with 30 mL of DMF and added to 120 mL of stirring deionized H_2O to cause a precipitate to fall out. The solid was collected via filtration and contained a mixture of products. Crude mass: 867.0 mg. The solid was dissolved in CH_2Cl_2 and chromatographed using silica gel.

***cis*-($\text{Re}_6\text{S}_8\text{Cl}_2(\text{PET}_3)_4]$ (*cis*-4).** This material was collected as the second band and was eluted with 20:1 $\text{CH}_2\text{Cl}_2/\text{CH}_3\text{CN}$ (yield: 219.3 mg, 19.1%). ^1H NMR (CD_2Cl_2 , ppm): 1.11 (36H, m, $\text{P}(\text{CH}_2\text{CH}_3)_3$), 2.05 and 2.12 (24H, m, $\text{P}(\text{CH}_2\text{CH}_3)_3$). ^{31}P $\{^1\text{H}\}$ NMR (CD_2Cl_2 , ppm): -16.77, -19.86. UV-vis (CH_3CN) nm (ϵ in $\text{M}^{-1}\text{cm}^{-1}$): 219 (70,800), 249 sh (19,900). MS (ESI(+)): m/z 1916.2 ($[\text{Re}_6\text{S}_8(\text{PET}_3)_4\text{Cl}_2]^+$). Anal. Calcd for $\text{C}_{24}\text{H}_{60}\text{P}_4\text{Cl}_2\text{Re}_6\text{S}_8$: C, 15.03; H, 3.15; N, 0.00. Found: C, 15.01; H, 3.01; N, 0.01.

***trans*-($\text{Re}_6\text{S}_8\text{Cl}_2(\text{PET}_3)_4]$ (*trans*-4).** This material was collected as the first band and was eluted with 40:1 $\text{CH}_2\text{Cl}_2/\text{CH}_3\text{CN}$ (yield: 124.5 mg, 10.8%). ^1H NMR (CD_2Cl_2 , ppm): 1.14 (36 H, m, $\text{P}(\text{CH}_2\text{CH}_3)_3$), 2.13 (24 H, m, $\text{P}(\text{CH}_2\text{CH}_3)_3$). ^{31}P $\{^1\text{H}\}$ NMR (CD_2Cl_2 , ppm): -16.15. UV-vis (CH_2Cl_2) nm (ϵ in $\text{M}^{-1}\text{cm}^{-1}$): 262 (18,800), 326 sh. MS (ESI(+)): m/z 1916.2 ($[\text{Re}_6\text{S}_8(\text{PET}_3)_4\text{Cl}_2]^+$). Anal. Calcd for $\text{C}_{24}\text{H}_{60}\text{P}_4\text{Cl}_2\text{Re}_6\text{S}_8$: C, 15.03; H, 3.15; N, 0.00. Found: C, 15.40; H, 3.18; N, 0.06.

X-ray Crystallography. (a). **General Procedures.** All single crystals were grown via the vapor diffusion technique using CH_3CN and toluene at -20 $^\circ\text{C}$. Crystals selected for diffraction experiments were coated with Paratone-N oil then placed under a cold N_2 gas stream on the diffractometer. Data for the *mer*-(Bu_4N) $[\text{Re}_6\text{S}_8(\text{PET}_3)_3\text{Cl}_3] \cdot 2\text{toluene}$ and *trans*-(Bu_4N) $_2$ $[\text{Re}_6\text{S}_8(\text{PET}_3)_2\text{Cl}_4] \cdot 3\text{toluene}$ structures were obtained using a Bruker SMART 1000 CCD detector/PLATFORM diffractometer with the crystals cooled to -80 $^\circ\text{C}$, while the data for the *fac*-(Bu_4N) $[\text{Re}_6\text{S}_8(\text{PET}_3)_3\text{Cl}_3] \cdot \text{NCCH}_3$ structure were obtained on a Bruker APEX II CCD detector/D8 diffractometer with the crystals cooled to -100 $^\circ\text{C}$. All diffraction measurements were obtained using

Table 1. Crystallographic Data

	<i>trans</i> -(Bu ₄ N) ₂ [Re ₆ S ₈ -(PEt ₃) ₂ Cl ₄]·3toluene	<i>mer</i> -(Bu ₄ N)[Re ₆ S ₈ -(PEt ₃) ₃ Cl ₃]·2toluene	<i>fac</i> -(Bu ₄ N)[Re ₆ S ₈ -(PEt ₃) ₃ Cl ₃]·MeCN
formula	C ₄₄ H ₁₀₂ Cl ₄ N ₂ P ₂ Re ₆ S ₈ ·3C ₇ H ₈	C ₃₄ H ₈₁ Cl ₃ NP ₃ Re ₆ S ₈ ·2C ₇ H ₈	C ₃₄ H ₈₁ Cl ₃ NP ₃ Re ₆ S ₈ ·NCCH ₃
FW (g·mol ⁻¹)	2513.10	2261.21	2117.99
space group	C2/c (No. 15)	<i>Pn</i> (alternate setting of <i>Pc</i> [No. 7])	<i>P2</i> ₁ / <i>c</i> (No. 14)
<i>a</i> (Å)	24.186(3)	15.4423(10)	16.3916(7)
<i>b</i> (Å)	19.144(2)	10.3485(7)	17.2370(8)
<i>c</i> (Å)	18.3863(19)	21.2933(14)	20.6159(9)
β (deg)	96.316(2)	95.0875(10)	92.7268(5)
<i>V</i> (Å ³)	8461.6(15)	3389.4(4)	5818.3(4)
<i>Z</i>	4	2	4
<i>T</i> (°C)	−80	−80	−100
radiation (λ (Å))	Mo Kα (0.71073)	Mo Kα (0.71073)	Mo Kα (0.71073)
ρ _{calcd} (g·cm ⁻³)	1.973	2.216	2.418
μ (mm ⁻¹)	8.946	11.13	12.96
Flack parameter		−0.002(5)	
<i>R</i> ₁ [<i>I</i> ≥ 2σ(<i>I</i>)]	0.0264	0.0282	0.0200
<i>wR</i> ₂ [all data]	0.0735	0.0519	0.0570
$R_1 = \sum F_o - F_c / \sum F_o $; $wR_2 = (\sum w(F_o^2 - F_c^2)^2 / \sum w(F_o^4))^{1/2}$.			

graphite-monochromated Mo Kα (λ = 0.71073 Å). All data were corrected for absorption by Gaussian integration after face-indexing and measurement of crystal dimensions.

The structures of *mer*-(Bu₄N)[Re₆S₈(PEt₃)₃Cl₃]·2toluene and *trans*-(Bu₄N)₂[Re₆S₈(PEt₃)₂Cl₄]·3toluene were solved via direct methods using SHELXS-97;²³ *fac*-(Bu₄N)[Re₆S₈(PEt₃)₃Cl₃]·NCCH₃ was solved using Patterson methods and structure expansion (DIRDIF-2008²⁴). Structures were refined by full-matrix least-squares on *F*² with SHELXL-97.²³ Hydrogen atoms were included as riding atoms and were placed in geometrically idealized positions with isotropic displacement parameters 120% of those of the U_{eq} for their parent atoms. See Table 1 for a summary of crystallographic data.

(b). Special Refinement Details. **(i). *trans*-(Bu₄N)₂[Re₆S₈-(PEt₃)₂Cl₄]·3toluene.** Two terminal carbons of an *n*-butyl group of the tetrabutylammonium ion were modeled as disordered, being split into two sets of atomic positions with occupancy factors of 60% (C35A, C36A) and 40% (C35B, C36B); the bond distances involving these carbons were constrained to be equal (within 0.03 Å) during refinement (i.e., *d*(C34–C35A) = *d*(C34–C35B) and *d*(C35A–C36A) = *d*(C35B–C36B)). The three solvent toluene molecules were each disordered, one about the crystallographic 2-fold axis (1/2, *y*, 1/4) and one each about the crystallographic inversion centers (1/4, 1/4, 1/2) and (0, 1/2, 0). For each toluene the atoms were refined with an occupancy factor of 50% and a common isotropic displacement parameter, the C_{methyl}–C_{ipso} distances were fixed at 1.52(1) Å, the C_{methyl}···C_{ortho} distances were fixed at 2.52(1) Å, and the ring carbons were refined as idealized hexagons with *d*_{C–C} = 1.39 Å and C–C–C angles of 120°.

(ii). *mer*-(Bu₄N)[Re₆S₈(PEt₃)₃Cl₃]·2toluene. One of the solvent toluene molecules was modeled as disordered, being split into two sets of atomic positions with occupancy factors of 60% (C20S, C21S, ..., C26S) and 40% (C30S, C31S, ..., C36S) and a common isotropic displacement parameter for all. Geometric restraints were applied as for the disordered toluene molecules of the *trans*-(Bu₄N)₂[Re₆S₈(PEt₃)₂Cl₄]·3toluene structure.

Luminescence Studies. Steady state emission spectra were obtained using a Perkin-Elmer LS55 fluorimeter equipped with a red-sensitive detector at excitation wavelengths that corresponded to the absorption wavelength of each compound in the blue region (420–490 nm). Excitation and emission slits were set to optimize the emission spectrum and the spectra were corrected for detector response. Emission quantum yields were

measured in the absence of oxygen (N₂ or Ar was bubbled through for 20 min prior to measurements being made) relative to a deoxygenated acetonitrile solution of [Mo₆(μ₃-Cl)₈Cl₆]^{2−} complex as a standard (φ_{em} = 0.19).^{4a} Index of refraction corrections were made for those complexes dissolved in dichloromethane. Time resolved emission signals were obtained upon sample excitation in the 420–480 nm range with a pulsed dye laser (PTI GL-302, Coumarin 456 dye as lasing medium) pumped by a nitrogen laser (337 nm, 5 Hz, PTI GL-3300). Light emitted from the sample was collected at 90 degree angle using a collimating lens system, passed through a monochromator set at a wavelength near the emission maximum (680–710 nm), and focused into a fast photomultiplier tube (PMT) light detector. The PMT signal was fed (50 Ω load) into a digital storage oscilloscope (100 MHz, Tektronix TDS1012). The average trace of at least 60 laser pulses was recorded and stored in a computer for further analysis. Time resolved experiments were carried out for air-saturated, deoxygenated, and oxygen-saturated samples to determine the effect of oxygen as a quencher of the luminescent state. Samples were saturated with oxygen by bubbling O₂ through the sample for 20 min prior to the measurements. All determinations were made at 296 ± 1 K.

Results and Discussion

Synthesis and Structures of [Re₆S₈(PEt₃)_{*n*}Cl_{6−*n*}]^{4−*n*} (*n* = 1–4). This report contains a detailed investigation involving the substitution chemistry of [Re₆S₈Cl₆]^{4−}. The chemistry is similar to substitution of the terminal halides in [Re₆S₈Br₆]^{4−} and [Re₆S₈I₆]^{3−}. However, the less labile chloride ligand allows for the preparation of the mono- and diphosphine complexes in good yields, 43% for **1** and 96% for [Re₆S₈-(PEt₃)₂Cl₄]^{2−} (*cis*-**2** and *trans*-**2** combined), which is not possible with the bromide and iodide analogues.^{17,18} Overall, substitution was controlled by varying the temperature and time of the reaction. Providing there were enough equivalents of phosphine to prepare the desired product, the duration of heating and the reaction temperature were found to be more important in determining the degree of substitution than the number of equivalents of phosphine. ³¹P NMR spectral data was used to help distinguish between stereoisomers. The disubstituted complexes, *cis*-**2** and *trans*-**2**, could not be distinguished in this manner; however, single crystals of *trans*-**2** were obtained enabling us to assign these accordingly.

[Re₆S₈(PEt₃)Cl₅]^{3−} is the first monophosphine hexarhenium chalcogenide cluster to be prepared; to the best of our knowledge, there is only one other example of a

(23) Sheldrick, G. M. *Acta Crystallogr.* **2008**, *A64*, 112–122.

(24) Beurskens, P. T.; de Gelder, R.; Smits, J. M. M.; Garcia-Granda, S.; Gould, R. O. *DIRDIF-2008 program system*; Crystallography Laboratory, Radboud University: Nijmegen, The Netherlands, 2008.

monosubstituted cluster of this type reported in the literature.²⁵ Even with substitution of the less labile chloride ligand, monosubstitution only required 1.5 h of heating at 100 °C. Thus, it is not surprising that a monophosphine complex was not prepared from either $[\text{Re}_6\text{S}_8\text{Br}_6]^{4-}$ or $[\text{Re}_6\text{Se}_8\text{I}_6]^{3-}$. The synthesis of the disubstituted complex, $[\text{Re}_6\text{S}_8(\text{PET}_3)_2\text{Cl}_4]^{2-}$ led to quantitative conversion (88% *cis*-2 and 8% *trans*-2) by the stereoisomers being separated via differences in solubility (alternatively, they could be separated using column chromatography). This high conversion to the disubstituted phosphine product has not been observed previously.^{17,18} The high yield of *cis*-2 in particular, is likely due to the lower reaction temperature (100 °C) leading to the formation of the statistically favored product.²⁶ The preparation of the triphosphine complexes, *mer*-3 and *fac*-3, are described in detail below. Heating $[\text{Re}_6\text{S}_8\text{Cl}_6]^{4-}$ at reflux for 3 days in the presence of excess phosphine led to the formation of the tetraphosphine complexes, although a substantial amount of the trisubstituted species was still present which resulted in low yields of *cis*-4 and *trans*-4 (these complexes were purified via column chromatography and can be distinguished via NMR spectroscopy). However, letting the reaction go for an additional 2 days almost doubled the yield of the tetrasubstituted product. As expected, *cis*-4 is generated in higher overall yield. After heating $[\text{Re}_6\text{S}_8\text{Cl}_6]^{4-}$ with 10 equiv of phosphine at reflux for 2 weeks, we observed two new peaks (in a 4:1 ratio) in the ^{31}P NMR spectrum indicating the formation of the pentasubstituted complex, $[\text{Re}_6\text{S}_8(\text{PET}_3)_5\text{Cl}]^-$; this compound made up about 10% of the reaction product (*cis*-4 and *trans*-4 were the major products). Because of the long reaction time we did not attempt to isolate the pentaphosphine product.

One reason we began examining the substitution chemistry of $[\text{Re}_6\text{S}_8\text{Cl}_6]^{4-}$ was to see if we could optimize the yield of the facial isomer, *fac*-3, to prepare larger quantities of this material for other studies. Although *fac*- $[\text{Re}_6\text{Se}_8(\text{PET}_3)_3\text{I}_3]^-$, and *fac*- $[\text{Re}_6\text{S}_8(\text{PET}_3)_3\text{Br}_3]^-$ were reported previously, at best they were obtained in 5% yield.^{17,18} We thought the less labile chloride ligand would allow us to prepare the facial isomer in higher yield. Our initial synthetic attempts involved heating $(\text{Bu}_4\text{N})_4[\text{Re}_6\text{S}_8\text{Cl}_6]$ and 3 equiv of PET_3 in DMF at reflux for 18 h, which led to a 25% yield of *mer*-3 and a negligible amount of *fac*-3. Since so little facial isomer was generated, we needed a different approach. Therefore, we tried starting with pure *cis*-2 instead of $[\text{Re}_6\text{S}_8\text{Cl}_6]^{4-}$, since a statistical substitution of the terminal chloride ligands on *cis*-2 should lead to 50% of *mer*-3 (substitution of either chloride *trans* to a PET_3) and 50% of *fac*-3 (substitution of either chloride *cis* to a PET_3). *Cis*-2 in DMF was heated at reflux with 2 equiv of PET_3 , and the reaction was monitored via ^{31}P NMR spectroscopy. Figure 1 shows the spectra obtained at different time intervals. Within 15 min both *mer*-3 and *fac*-3 are observed. Over time, the disubstituted species decrease in concentration, while the amounts of the trisubstituted products increase, with the maximum yield occurring at 3 h (the tetraphosphine products start to form after 3 h). One important thing to note is that even though

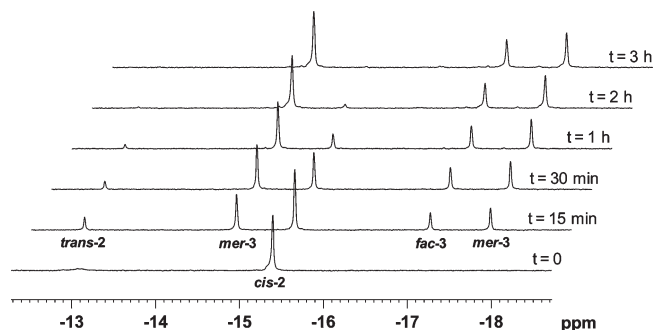


Figure 1. 202.5 MHz $^{31}\text{P}\{^1\text{H}\}$ spectral data of samples taken at different time intervals in the reaction of *cis*- $[\text{Re}_6\text{S}_8(\text{PET}_3)_2\text{Cl}_4]^{2-}$ with 2 equiv of PET_3 in DMF at reflux.

cis-2 was pure to begin with, after heating at reflux for 15 min some *trans*-2 was observed, indicating that an isomerization reaction (*cis*- to *trans*-) was taking place. The higher temperature reaction conditions seems to be responsible for this conversion, indicating that the thermodynamically stable isomer of the diphosphine product contains a *trans* arrangement of the phosphine ligands; this isomer is likely favored for steric reasons. Even with a small amount of *trans*-2 forming at the beginning of the reaction, we still expected to generate *mer*-3 and *fac*-3 in approximately the same amounts. However, a non-decoupled ^{31}P NMR spectrum taken at 3 h integrates for 2:1 ratio of *mer*-3:*fac*-3. Therefore, it is possible that isomerization of the trisubstituted cluster complex is occurring as well. The yield of the crude product (after removal of the DMF and reprecipitation) was 97%, and once purified, the isolated yields were 52% of *mer*-3 and 19% of *fac*-3. This is the highest yield reported for the preparation of a facial isomer of a $[\text{Re}_6\text{Q}_8]^{2+}$ based cluster in solution.²⁷ In addition, evidence of phosphine isomerization indicates that these ligands may not form as strong a bond with rhenium as originally thought.

The rearrangement of ligands coordinated to polynuclear metal complexes has been studied for some time.²⁸ Many of the studies reported to date focus on fluxional transition metal carbonyl clusters, or clusters containing analogous ligands (i.e., NO or CNR) which can easily bridge two metal centers. The various mechanisms for ligand rearrangement are typically classified by molecularity, that is, intramolecular or intermolecular.²⁹ Because of the regular geometry and rigidity of the $[\text{Re}_6\text{S}_8]^{2+}$ cluster core, it is doubtful that the isomerization described here is due to an intramolecular process. More than likely, the process involves dissociation of one or more of the terminal ligands (unlike substitution at a single metal center, the loss of a single ligand will not lead to a change in the geometry of the cluster). Further studies

(27) Fedorov and co-workers report the solid state synthesis of the mixed core complex *fac*- $[\text{Re}_6(\mu_3\text{-Q})_7(\mu_3\text{-Br})(\text{PPh}_3)_3\text{Br}_3]$ (Q = S, Se) in high yield. Shestopalov, M. A.; Mironov, Y. V.; Brylev, K. A.; Kozlova, S. G.; Fedorov, V. E.; Spies, H.; Pietzsch, H.-J.; Stephan, H.; Geipel, G.; Bernhard, G. *J. Am. Chem. Soc.* **2007**, *129*, 3714–3721.

(28) (a) Band, E.; Muettterties, E. L. *Chem. Rev.* **1978**, *78*, 639–658. (b) Bradford, A. M.; Douglas, G.; Manojlovic-Muir, L.; Muir, K. W.; Puddephatt, R. J. *Organometallics* **1990**, *9*, 409–416. (c) Adams, R. D.; Captain, B.; Fu, W.; Pellechia, P. J. *Chem. Commun.* **2000**, 937–938. (d) Adams, R. D.; Captain, B.; Fu, W.; Pellechia, P. J. *Inorg. Chem.* **2003**, *32*, 3111–3118. (e) Bradford, A. M.; Jennings, M. C.; Puddephatt, R. J. *Organometallics* **1988**, *7*, 792–793.

(29) Wilkins, R. G. *Kinetics and Mechanism of Reactions of Transition Metal Complexes*, 2nd ed.; VCH Publishers, Inc.: New York, 1991; pp 333–368.

(25) Choi, S.-J.; Brylev, K. A.; Xu, J.-Z.; Mironov, Y. V.; Fedorov, V. E.; Sohn, Y. S.; Kim, S.-J.; Choy, J.-H. *J. Inorg. Biochem.* **2008**, *102*, 1991–1996.

(26) *Cis*-2 is statistically favored because there are four chloride ligands *cis*- to the PET_3 ligand in **1**, and only one chloride ligand *trans*- to the PET_3 in **1**.

Table 2. Selected Bond Lengths (Å) and Bond Angles (deg) for (Bu₄N)₂[*trans*-Re₆S₈(PEt₃)₂Cl₄]·3toluene, (Bu₄N)[*mer*-Re₆S₈(PEt₃)₃Cl₃]·2toluene, and (Bu₄N)[*fac*-Re₆S₈(PEt₃)₃Cl₃]·MeCN

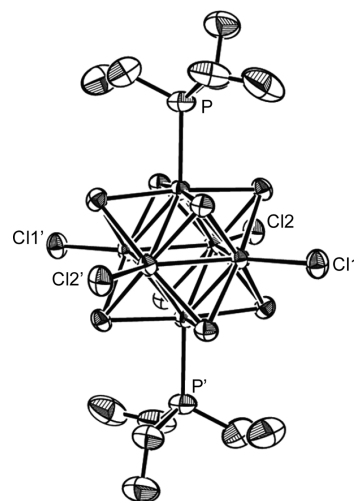
	(Bu ₄ N) ₂ <i>trans</i> - 2 •3toluene	(Bu ₄ N) <i>mer</i> - 3 •2toluene	(Bu ₄ N) <i>fac</i> - 3 •MeCN
Re–Re	2.5954(3)–2.6083(3)	2.5942(4)–2.6115(4)	2.5975(2)–2.6101(2)
mean	2.600(2)	2.604(2)	2.604(1)
Re–S	2.3956(11)–2.4144(12)	2.3951(19)–2.4193(19)	2.4012(11)–2.414(11)
mean	2.406(2)	2.408(2)	2.407(1)
Re–Cl	2.4317(12), 2.4321(12)	2.421(2)–2.431(2)	2.4189(11)–2.4407(11)
mean		2.426(3)	2.433(7)
Re–P	2.4690(14)	2.468(2)–2.472(2)	2.4676(11)–2.4694(11)
mean		2.470(2)	2.468(1)
Re–Re–Re ^a	59.818(8)–60.311(7)	59.705(12)–60.322(12)	59.753(7)–60.163(6)
mean	60.00(5)	60.00(4)	60.00(3)
Re–Re–Re ^b	89.568(11)–90.432(11)	89.529(13)–90.461(13)	89.757(8)–90.183(8)
mean	90.00(15)	90.00(9)	90.00(3)
Re–Re–S	56.99(3)–57.62(3)	56.88(5)–57.71(5)	57.02(3)–57.56(3)
mean	57.30(4)	57.28(3)	57.26(2)
Re–Re–S	116.82(3)–117.87(3)	116.74(5)–117.99(5)	116.82(3)–117.6(3)
mean	117.26(7)	117.24(4)	117.22(2)
S–Re–S	89.28(4)–90.29(4)	89.15(7)–90.55(7)	89.26(4)–90.47(4)
mean	89.8(1)	89.80(8)	89.80(7)
S–Re–S	172.85(4)–174.14(4)	172.61(7)–173.89(7)	172.98(4)–173.55(4)
mean	173.3(3)	173.26(13)	173.23(4)
Re–S–Re	65.21(3)–65.58(3)	64.99(5)–65.93(5)	65.14(3)–65.66(3)
mean	65.41(3)	65.45(4)	65.48(3)

^a Within triangular faces. ^b Within equatorial squares.

need to be conducted to verify that dissociation is the rate determining step, and to elucidate a detailed mechanism of this isomerization process.

Structure Analysis. Single crystals of complexes **1**, *trans*-**2**, *mer*-**3**, and *fac*-**3** were grown for X-ray diffraction analyses. Crystals of compound **1** were found to be weakly diffracting; therefore, only the structures of *trans*-**2**, *mer*-**3**, and *fac*-**3** are reported here. Table 2 contains selected interatomic bond distances and angles, along with average values, and Figures 2 and 3 contain the ORTEP diagrams of these three complexes. Key bond lengths (Re–Re and Re–S) and angles (Re–Re–Re, Re–Re–S, S–Re–S, and Re–S–Re) within the cluster core are typical for [Re₆S₈]²⁺ based cluster complexes.³⁰ In addition, the terminal Re–Cl bonds with lengths of 2.4317(12) and 2.4321(12) for *trans*-**2**, 2.421(2), 2.425(2), and 2.431(2) for *mer*-**3**, and 2.4189(11), 2.4387(11), and 2.4407(11) for *fac*-**3** are in the middle of the range observed for hexarhenium chalcogenide cluster complexes,^{5b,21} as are the Re–P bond distances.^{17,18,31}

Electrochemical Studies. The electrochemical properties of these new cluster complexes were investigated using cyclic voltammetry. Complexes **1**, *cis*-**2**, *trans*-**2**, *mer*-**3**, and *fac*-**3**

**Figure 2.** ORTEP diagram of *trans*-[Re₆S₈(PEt₃)₂Cl₄]²⁻. H atoms omitted for clarity and ellipsoids at 50% probability.

display two redox processes in MeCN; the first is a reversible couple, and the second, appearing at approximately 0.86 V more positive than that of the first couple, is irreversible. The tetrasubstituted complexes, *cis*-**4** and *trans*-**4**, were not that soluble in MeCN. Therefore, the electrochemical data for these compounds was recorded in CH₂Cl₂. Only the reversible couple was observed for these two complexes, which is likely because methylene chloride has a smaller voltage window than MeCN, and thus, we were unable to access the second redox process. All redox potentials are listed in Table 3, and cyclic voltammograms of all newly

(30) See references 2d, 5b, 18, and 21a along with the following: (a) Brylev, K. A.; Naumov, N. G.; Peris, G.; Llusar, R.; Fedorov, V. E. *Polyhedron* **2003**, *22*, 3383–3387. (b) Baudron, S. A.; Deluzet, A.; Boubekeur, K.; Batail, P. *Chem. Commun.* **2002**, 2124–2125. (c) Dorson, F.; Molard, Y.; Cordier, S.; Fabre, B.; Efremova, O.; Rondeau, D.; Mironov, Y.; Circu, V.; Naumov, N.; Perrin, C. *Dalton Trans.* **2009**, 1297–1299. (d) Brylev, K. A.; Mironov, Y. V.; Kozlova, S. G.; Fedorov, V. E.; Kim, S.-J.; Pietzsch, H.-J.; Stephan, H.; Ito, A.; Ishizaka, S.; Kitamura, N. *Inorg. Chem.* **2009**, *48*, 2309–2315.

(31) Decker, A.; Simon, F.; Boubekeur, K.; Fenske, D.; Batail, P. *Z. Anorg. Allg. Chem.* **2000**, *626*, 309–313.

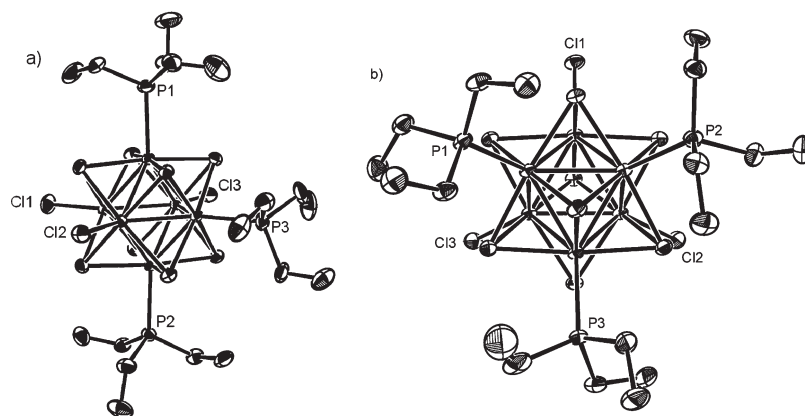


Figure 3. ORTEP diagrams of (a) $\text{mer-}[\text{Re}_6\text{S}_8(\text{PEt}_3)_3\text{Cl}_3]^-$ and (b) $\text{fac-}[\text{Re}_6\text{S}_8(\text{PEt}_3)_3\text{Cl}_3]^-$. H atoms omitted for clarity and ellipsoids at 50% probability.

Table 3. Electrochemical Data for the $[\text{Re}_6\text{S}_8(\text{PEt}_3)_n\text{Cl}_{6-n}]^{4-n}$ ($n = 0-4$) Series of Complexes^a

complex	$E_{1/2}$, V	$E_{p,a}$, V
$(\text{Bu}_4\text{N})_4[\text{Re}_6\text{S}_8\text{Cl}_6]^b$	-0.093	0.767 ^c
$(\text{Bu}_4\text{N})_3[\text{Re}_6\text{S}_8(\text{PEt}_3)\text{Cl}_5]$ (1)	0.070	0.948
$(\text{Bu}_4\text{N})_2[\text{cis-Re}_6\text{S}_8(\text{PEt}_3)_2\text{Cl}_4]$ (cis-2)	0.234	1.114
$(\text{Bu}_4\text{N})_2[\text{trans-Re}_6\text{S}_8(\text{PEt}_3)_2\text{Cl}_4]$ (trans-2)	0.235	1.111
$(\text{Bu}_4\text{N})[\text{mer-Re}_6\text{S}_8(\text{PEt}_3)_3\text{Cl}_3]$ (mer-3)	0.389	1.239
$(\text{Bu}_4\text{N})[\text{fac-Re}_6\text{S}_8(\text{PEt}_3)_3\text{Cl}_3]$ (fac-3)	0.401	1.230
$\text{cis-}[\text{Re}_6\text{S}_8(\text{PEt}_3)_4\text{Cl}_2]$ (cis-4) ^d	0.572	
$\text{trans-}[\text{Re}_6\text{S}_8(\text{PEt}_3)_4\text{Cl}_2]$ (trans-4) ^d	0.550	

^a All potentials referenced to the $\text{FcP}_2^+/\text{FcP}_2$ couple. ^b See text for comparison between these values and previously published values. ^c Reversible couple ($E_{1/2}$ value). ^d CV data was measured in CH_2Cl_2 and then adjusted to MeCN for solvent effects based on the observed potential shift of the $\text{FcP}_2^+/\text{FcP}_2$ couple in the same solvents. $E_{p,a}$ value of the second redox process could not be measured.

reported complexes can be found in the Supporting Information (Figures S1–S6). Included in Table 3 is our data for the hexachloro complex, $(\text{Bu}_4\text{N})_4[\text{Re}_6\text{S}_8\text{Cl}_6]$; the data for this complex matches that reported by Holm and co-workers^{2d} as well as that reported by Yoshimura et al. once adjustments for the different reference electrodes are made.^{5b} The two couples (-0.093 and 0.767 V) of the $[\text{Re}_6\text{S}_8\text{Cl}_6]^{4-}$ complex have been assigned to $\text{Re}^{\text{III}}_5\text{Re}^{\text{IV}}/\text{Re}^{\text{III}}_6$ and $\text{Re}^{\text{III}}_4\text{Re}^{\text{IV}}_2/\text{Re}^{\text{III}}_5\text{Re}^{\text{IV}}$, respectively.

On the basis of the difference between the two reversible couples of $[\text{Re}_6\text{S}_8\text{Cl}_6]^{4-}$ is 0.86 V (irrespective of the reference), which is approximately the same value we observed between the $E_{1/2}$ and the $E_{p,a}$ of the newly reported complexes, we assign the reversible wave to the $\text{Re}^{\text{III}}_5\text{Re}^{\text{IV}}/\text{Re}^{\text{III}}_6$ couple and the irreversible process to the oxidation of $\text{Re}^{\text{III}}_5\text{Re}^{\text{IV}}$ to $\text{Re}^{\text{III}}_4\text{Re}^{\text{IV}}_2$. The rest potential was measured to verify the oxidation state of the cluster complexes in solution. In all cases, the rest potential was 0.150 V (at a minimum) lower than the $E_{p,a}$ of the first redox couple, indicating that Re^{III}_6 was the predominant species in solution.

Our data nicely demonstrates the impact of substituting the terminal chloride ligands with PEt_3 on the electronic properties of the cluster. As expected, the substitution of an anionic chloride ligand for a neutral phosphine ligand results in a complex that is more difficult to oxidize. Plotting the $E_{1/2}$ of the reversible couple versus the number of phosphine ligands on the cluster complex, leads to a linear plot ($R^2 = 0.9991$) with a slope of 0.163 V/(number of PEt_3 ligands), see Figure S7 in the Supporting Information.

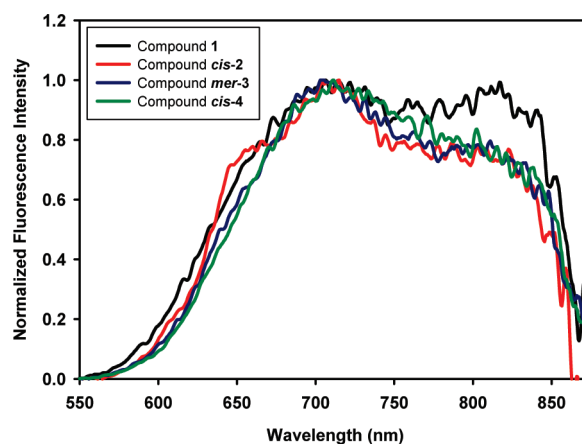


Figure 4. Emission spectra of $[\text{Re}_6\text{S}_8(\text{PEt}_3)_n\text{Cl}_{6-n}]^{4-n}$ clusters $n = 1$ (**1**), $n = 2$ (**cis-2**), $n = 3$ (**mer-3**), and $n = 4$ (**cis-4**). The emission spectra for the remaining compounds (**trans-2**, **fac-3**, and **trans-4**) can be found in the Supporting Information (Figure S8).

Luminescence Studies. Figure 4 shows the emission spectra of the compounds. All compounds show a broad emission in the $560-880$ nm range. There is no clear correlation between the emission maximum peak wavelength and the number of PEt_3 substituents, although the band origin (short wavelength tail) seems to red shift with an increase of the number of phosphines. Table 4 contains relative emission yields (ϕ_{em}), radiative lifetimes (τ_0), and oxygen quenching rate constants (k_q). Emission yields are comparable to those previously reported for the hexachloro and hexaphosphine complexes. Although they do not seem to follow any particular trend with the number of phosphine substituents, an increase in the number of phosphine ligands favors light emission. Radiative lifetimes, which were obtained from the light emission decay rate constants, are affected by the number of phosphine ligands, varying from $7 \mu\text{s}$ in the tetraphosphine complexes down to $4 \mu\text{s}$ for the monophosphine complex. Thus, the general trend is an increase in the excited state lifetime with the replacement of the electron rich halides with neutral triethylphosphine ligands. This general trend of increasing excited state lifetime as halides are replaced with phosphine ligands has been observed previously by Sasaki and co-workers for various $[\text{Re}_6\text{Se}_8]^{2+}$ based clusters containing different η^1 - and η^2 -diphosphine ligands, as well as by Gray et al.

Table 4. Photophysical Parameters of $[\text{Re}_6\text{S}_8(\text{PET}_3)_n\text{Cl}_{6-n}]^{4-n}$ Clusters

complex	$\phi_{\text{em}}^{b,e}$	τ_0 (μs)	λ_{em} (nm)	k_r ($\times 10^3 \text{ s}^{-1}$)	k_{nr} ($\times 10^5 \text{ s}^{-1}$)	k_q ($\times 10^7 \text{ M}^{-1} \text{ s}^{-1}$)	solvent
$[\text{Re}_6\text{S}_8\text{Cl}_6]^{4-a}$	0.035	5.7	762	6.1	1.69	10.2 ^d	CH_3CN
1	0.038	4.13	713	9.2	2.33	6.29	CH_3CN
<i>cis</i> - 2	0.041	5.60	714	7.3	1.71	4.45	CH_3CN
<i>trans</i> - 2	0.036	4.74	710	7.6	2.03	4.51	CH_3CN
<i>mer</i> - 3	0.038	5.68	703	6.7	1.69	3.43	CH_3CN
<i>fac</i> - 3	0.041	7.11	711	5.8	1.35	2.96	CH_3CN
<i>cis</i> - 4	0.049	6.61	722	7.4	1.44	1.25	CH_2Cl_2
<i>trans</i> - 4	0.042	7.01	717	6.0	1.37	1.07	CH_2Cl_2
$[\text{Re}_6\text{S}_8(\text{PET}_3)_6]^{2+c}$	0.044	10.0	719	4.4	0.956		CH_2Cl_2

^a. Average from refs 4a and 5a. ^b. Relative to $[\text{Mo}_6(\mu_3\text{-Cl})_8\text{Cl}_6]^{2-}$ in deoxygenated MeCN solution. ^c. Reference 4a. ^d. This work. ^e. Data for *cis*-**4** and *trans*-**4** was corrected for the index of refraction.

for the $[\text{Re}_6\text{S}_8(\text{PET}_3)_n\text{Br}_{6-n}]^{4-n}$ ($n = 3-6$) and $[\text{Re}_6\text{Se}_8(\text{PET}_3)_n\text{I}_{6-n}]^{4-n}$ ($n = 4-6$) series of complexes.^{32,4a}

A direct comparison of the chlorinated complexes with their equivalent brominated analogues reveals that the chlorinated complexes have longer lifetimes (by 1–2 μs). This observation is also consistent with the previous result in the $[\text{Re}_6\text{S}_8\text{X}_6]^{4-}$ ($\text{X} = \text{Cl}, \text{Br}, \text{I}$) complexes.^{4a,5a} The increase in the polarizability of the ligand (i.e., ability to donate electron density) decreases the lifetime of the excited state.

It is possible to obtain the rate constants for radiative (k_r) and non-radiative (k_{nr}) relaxation from the emission yields and lifetimes:

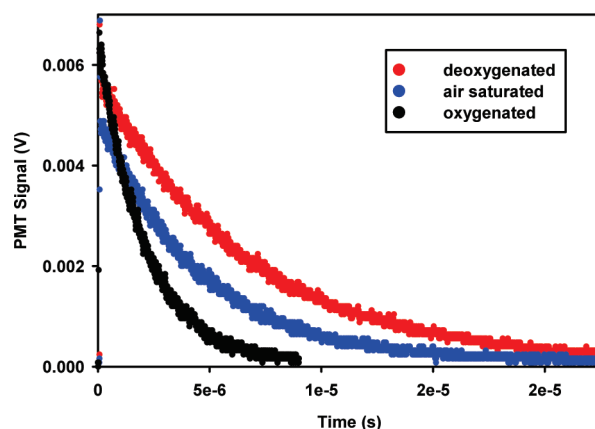
$$k_r = \frac{\phi_{\text{em}}}{\tau_0} \quad k_{\text{nr}} = \frac{(1 - \phi_{\text{em}})}{\tau_0} \quad (1,2)$$

These values are also included in Table 4. As expected from the relative low emission yields, relaxation of the emitting excited state occurs preferably by a non-radiative relaxation pathway. On average, the rates of non-radiative relaxation are about 25 times larger than radiative rates for all complexes. In comparison, the bromide and iodide analogues show a larger difference between the non-radiative and radiative rates (e.g., $k_{\text{nr}}/k_r = 124$ for *trans*- $[\text{Re}_6\text{S}_8(\text{PET}_3)_4\text{Br}_2]$), and the non-radiative relaxation rates for bromide and iodide compounds are consistently larger ($\sim 1.2-1.5$ times) than for the chlorinated compounds along the series. The replacement of chloride with triethylphosphine slows down both non-radiative and radiative relaxation causing the excited state to live longer and to emit light more efficiently.

We also studied the effect of molecular oxygen on the relaxation rates. Since the excited state is a triplet state, the reaction with molecular oxygen (also in a triplet state) is expected to be efficient.³³ Figure 5 illustrates typical time-resolved traces as a function of oxygen content in the solution. Clearly the decay of the excited luminescent state is affected by the presence of oxygen, confirming that the luminescent state has a triplet state character. Stern–Volmer quenching plots are linear (see Figure S9, Supporting Information) and allow for the determination of the bimolecular quenching constant k_q according to:

$$k_{\text{obs}} = k_0 + k_q[\text{O}_2] \quad (3)$$

Values of the quenching rate constant are included in Table 4. The quenching of the luminescent state by oxygen

**Figure 5.** Effect of oxygen concentration on the emission decay of *fac*- $[\text{Re}_6\text{S}_8(\text{PET}_3)_3\text{Cl}_3]^-$ (*fac*-**3**) in acetonitrile solution.

is slower than by other electron acceptors previously studied.³⁴ It must be noted that the rate of quenching is dependent on the number of triethylphosphine ligands, varying from $1.02 \times 10^8 \text{ M}^{-1} \text{ s}^{-1}$ for the cluster without phosphine ligands to $1.07 \times 10^7 \text{ M}^{-1} \text{ s}^{-1}$ for the one with four phosphine ligands. Thus an increase in the number of triethylphosphine ligands induces a decrease of the bimolecular oxygen quenching rate. This effect seems to correlate with the increasing trend of the emission lifetime in the absence of oxygen (i.e., τ_0) and the decreasing trend in the non-radiative rates (k_{nr}). The results clearly indicate that the presence of PET_3 ligands decreases the reactivity of the triplet state and extends its lifetime. It is well established that the presence of the electron acceptor ligands perturb the photophysical properties of the emitting $[\text{Re}_6\text{S}_8]^{2+}$ core.^{21b} Previous experimental and theoretical studies indicate that the mixing of the ligand orbitals with the metal-chalcogen core occurs via a metal-to-ligand charge-transfer (MLCT) mechanism.^{21b} The stabilization of the luminescent state by the phosphine ligands is also supported by the trend in the $E_{1/2}$ values. The replacement of chloride ligands with PET_3 makes $E_{1/2}$ more positive indicating ground state stabilization of the cluster core by the less electron rich PET_3 ligand. Interestingly, there is a correlation between the $E_{1/2}$ and k_q , which is expected if the quenching mechanism by oxygen is dependent on electron transfer. Quenching of the excited state by oxygen may occur via energy transfer and electron transfer mechanisms to produce reactive oxygen species, singlet oxygen and superoxide. Marcus theory may be used

(32) (a) Chen, Z.-N.; Yoshimura, T.; Abe, M.; Sasaki, Y.; Ishizaka, S.; Kim, H.-B.; Kitamura, N. *Angew. Chem., Int. Ed.* **2001**, *40*, 239–242. (b) Chen, Z.-N.; Yoshimura, T.; Abe, M.; Tsuge, K.; Sasaki, Y.; Ishizaka, S.; Kim, H.-B.; Kitamura, N. *Chem.—Eur. J.* **2001**, *7*, 4447–4455.

(33) Yoshimura, T.; Matsuda, A.; Ito, Y.; Ishizaka, S.; Shinoda, S.; Tsukube, H.; Kitamura, N.; Shinohara, A. *Inorg. Chem.* **2010**, *49*, 3473–3481.

(34) Kobayashi, N.; Ishizaka, S.; Yoshimura, T.; Kim, H.-B.; Sasaki, Y.; Kitamura, N. *Chem. Lett.* **2000**, 234–235.

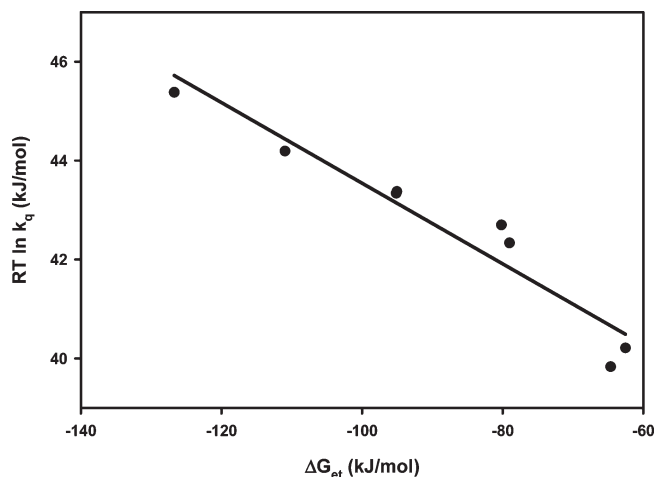


Figure 6. Correlation between the bimolecular oxygen quenching rate constant and the electron transfer free energy for the $[\text{Re}_6\text{S}_8(\text{PEt}_3)_n\text{Cl}_{6-n}]^{4-n}$ series of complexes.

to correlate the free energy of electron transfer (ΔG_{et}) and the oxygen quenching rate constant (as $RT \ln k_q$).³⁵ If electron transfer were the exclusive quenching mechanism by oxygen, a linear correlation with a slope equal to -0.50 is expected. ΔG_{et} can be estimated from the difference between the $E_{1/2}$ of the cluster and the reduction potential of molecular oxygen into superoxide ($E(\text{O}_2/\text{O}_2^-)$), offset by the energy difference between the excited and ground states of the cluster (ΔE_{0-0}).^{34,35}

$$\Delta G_{et} = 96.5[E_{1/2} - E(\text{O}_2/\text{O}_2^-)] - \Delta E_{0-0} \quad (4)$$

ΔE_{0-0} is estimated from the short-wavelength tail of the emission spectrum.³⁶ Because of the small spectral differences between the clusters in this study, a value of 202 kJ/mol was used for all of them. Figure 6 shows the correlation between the estimated ΔG_{et} and $RT \ln k_q$; a linear fit yields an R^2 of 0.924 and a slope of -0.082 . Deviation from the predicted linear behavior and the theoretical slope of -0.50 suggests that both energy and electron transfer mechanisms are involved. Similar results were obtained previously for the related hexanuclear tungsten and molybdenum halide clusters.³⁵

Conclusions

The terminal chloride ligands of the $[\text{Re}_6\text{S}_8\text{Cl}_6]^{4-}$ cluster have been substituted leading to the preparation of a new series of complexes, $[\text{Re}_6\text{S}_8(\text{PEt}_3)_n\text{Cl}_{6-n}]^{4-n}$ ($n = 1-4$). This includes

(35) Jackson, J.; Turro, C.; Newsham, M. D.; Nocera, D. G. *J. Phys. Chem.* **1990**, *94*, 4500–4507.

(36) Adamson, A. W. *J. Chem. Educ.* **1983**, *60*, 797–802.

isolation of the different isomers generated when two or more phosphine ligands were coordinated, and the highest yield reported to date for *fac*- $[\text{Re}_6\text{Q}_8(\text{PEt}_3)_3\text{X}_3]^-$ ($\text{Q} = \text{S}$ or Se and $\text{X} = \text{Cl}$, Br , or I). The substitution chemistry of $[\text{Re}_6\text{S}_8\text{Cl}_6]^{4-}$ was found to be similar to that of $[\text{Re}_6\text{Q}_8]^{2+}$ containing terminal bromide and iodide ligands. However, the chloride ligand is considerably less labile which allowed for the preparation of first monophosphine complex, $[\text{Re}_6\text{S}_8(\text{PEt}_3)\text{Cl}_5]^{3-}$ and higher yields of the diphosphine complexes. Even though chloride and triethylphosphine are considered inert when bonded to these hexarhenium clusters, we observed an isomerization reaction taking place between the *cis*- and *trans*-isomers of $[\text{Re}_6\text{S}_8(\text{PEt}_3)_2\text{Cl}_4]^{2-}$, and between the *fac*- and *mer*-isomers of $[\text{Re}_6\text{S}_8(\text{PEt}_3)_3\text{Cl}_3]^-$ at elevated temperatures. The diphosphine isomer **trans-2** and the triphosphine isomer **mer-3** are likely favored because of steric reasons. This is the first report of such an isomerization reaction involving these hexarhenium clusters.

The electrochemical and luminescent properties of these complexes also proved quite interesting. All complexes emit between 560–880 nm with excited state lifetimes ranging from 4.13 to 7.11 μs , and replacement of chloride by PEt_3 around the cluster core increases the stability of the luminescent state relative to quenching by molecular oxygen. The presence of phosphine ligands slows down both radiative and non-radiative decay, while oxygen quenches the excited state in a manner dependent on the number of phosphine ligands. The oxygen quenching rate decreases with an increase in the number of phosphine ligands, confirming the stabilizing effect of PEt_3 in the excited state. Weak correlation between ΔG_{et} and k_q on the basis of Marcus theory for electron transfer indicates that oxygen quenching does not occur exclusively via electron transfer and that it most likely occurs via a combination of electron and energy transfer. This study demonstrates the utility of $[\text{Re}_6\text{S}_8\text{Cl}_6]^{4-}$ in the preparation of site-differentiated systems, and provides insight into the nature of the luminescent excited state via quenching experiments.

Acknowledgment. This research was supported by the NSF (CAREER-0239805 and CHE 0957729). The Bruker Avance III NMR spectrometer was also obtained with funds from the NSF (CHE-0722385).

Supporting Information Available: Cyclic voltammograms of all compounds (Figures S1–S6), a plot of the $E_{1/2}$ versus number of coordinated PEt_3 ligands (Figure S7), the emission spectra of **trans-2**, **fac-3**, and **trans-4** (Figure S8), Stern–Volmer emission quenching plots (Figure S9), and UV–vis spectra of all compounds (Figures S10–S12). The X-ray crystallographic files in CIF format for the Bu_4N^+ salts of **trans-2**·3toluene, **mer-3**·2toluene, and **fac-3**·MeCN are also included. This material is available free of charge via the Internet at <http://pubs.acs.org>.